Inorganica Chimica Acta 373 (2011) 85–92

Contents lists available at ScienceDirect

Inorganica Chimica Acta

journal homepage: www.elsevier.com/locate/ica

Synthesis and characterization of four cubical molybdenum(V) tetramers and their catalytic properties for the epoxidation of *cis*-cyclooctene using H_2O_2

Linsheng Feng, John S. Maass, Rudy L. Luck *

Department of Chemistry, Michigan Technological University, 1400 Townsend Drive, Houghton, MI 49931, USA

A R T I C L E I N F O

Article history:
Received 28 January 2011
Received in revised form 20 March 2011
Accepted 26 March 2011
Available online 1 April 2011

Keywords:
Molybdenum tetramer
Distorted cube
X-ray crystal structures
Organophosphinic acid
Epoxidation
cis-Cyclooctene

A B S T R A C T

Molybdenum tetramers: $Mo_4(\mu^3\text{-}O)_4[\mu\text{-}O_2P(CH_2Cl)_2]_4O_4$ (**1**), $Mo_4(\mu^3\text{-}O)_4(\mu\text{-}O_2P(CH_2OH)_2)_4O_4$ (**2**), $Mo_4(\mu^3\text{-}O)_4[\mu\text{-}O_2P(PhOMe)_2]_4O_4$ (**3**), and $Mo_4(\mu^3\text{-}O)_4[\mu\text{-}O_2P(o\text{-}C_6H_4(CH_2)_2)]_4O_4$ (**4**) have been synthesized and characterized by IR, UV–Vis, and ^{31}P NMR spectroscopy. Molybdenum tetramers **1** and **4** along with the ligands **L2A** and **L4** were structurally characterized by single crystal X-ray crystallography. An infinite 2D polymeric sheet was formed via inter and intra hydrogen bonds in the crystals of **L2A**. The crystals of **L4** consist of infinite polymeric chains formed through hydrogen bonding. All molybdenum tetramers were tested as catalysts for the epoxidation of *cis*-cyclooctene in the presence of H_2O_2. Compounds **1** and **2** resulted in more than 80% epoxide after 24 hours at 70 °C, and displayed superior catalytic activities over compounds **3** and **4** under identical conditions. The superior catalytic activities of compounds **1** and **2** may be attributed to their better solubility in the ethanol/H_2O_2 system.

1. Introduction

Epoxides are an important source of starting materials in industry and drug discovery [1]. A common method for producing epoxides from olefins is to react them with oxidants such as hydrogen peroxide, oxygen, or alkyl hydroperoxides in the presence of a high-valent transition-metal catalyst [2]. In particular, molybdenum and tungsten complexes have been widely investigated because of their high activity for the epoxidation of olefins using tert-butyl hydroperoxide (TBHP) or hydrogen peroxide [2–17]. The use of hydrogen peroxide is ideal because of its high atom-efficiency as compared to TBHP and that the sole byproduct, water, is environmentally benign [18,19]. The use of chlorinated solvents for the epoxidation of olefins is becoming increasing unacceptable because of their negative environmental effect [20]. Catalytic systems using environmentally friendly solvents such as ethanol or acetonitrile are being developed to replace the chlorinated solvent systems [11]. In general, the epoxidation of olefins using transition metal catalysts with hydrogen peroxide in non-chlorinated solvents is a very active area in chemistry.

Cubical compounds $M_4(\mu^3\text{-}X)_4$, where M = Co, Fe, Mo, Mn and X = O or S have drawn interest not only for their unique structures and electronic properties, but also for their potential applications in catalysis [21,22]. Molybdenum cubical-like structures such as $[Mo_4(\mu^3\text{-}X)_4O_4]^{4+}$, X = S or O have been synthesized before [23–25]. These compounds all contain distorted cubane core arrangements which result from the formation of Mo–Mo single bonds with Mo(V) atoms and the ability of the S^{2-} and O^{2-} anions to act as triply bridging ligands [23,26]. These cubic arrangements are stabilized by various ligands such as the monodentate dimethylamine and trimethylsilyloxy [26] and the bidentate bridging 3,4-dihydroxycyclobut-3-ene-1,2-dione [27], phosphate [25,28], dimethylthiophosphinato [29], diphenylphosphinato [24], and dimethylphosphinato [30]. In this paper, we extend this class of compounds using di(chloromethyl)phosphinic acid (**L1**), di(hydroxymethyl)phosphinic acid (**L2**), di(p-methoxyphenyl)-phosphinic acid (**L3**) and 2-hydroxyisophosphindoline-2-oxide (**L4**) as ligands to synthesize new molybdenum(V) tetramers **1**–**4**, Scheme 1. Compounds **1**–**4** were characterized by IR, UV–Vis and NMR spectroscopic methods. The structure of the ligands **L2A** and **L4** and compounds **1** and **4** were determined by single X-ray diffraction. The catalytic capabilities of compounds **1**–**4** for the epoxidation of *cis*-cyclooctene were assessed using hydrogen peroxide as the source of oxygen.

2. Experimental

2.1. General method

Infrared spectra were obtained on a PerkinElmer Spectrum one FT-IR spectrometer. ^{31}P NMR data were recorded on a Varian XL-400 spectrometer. A Fisher–Johns melting point apparatus (Fisher Scientific Company) was used for the melting point determina-

---

* Corresponding author.
E-mail address: rluck@mtu.edu (R.L. Luck).

0020-1693/$ - see front matter © 2011 Elsevier B.V. All rights reserved.
doi:10.1016/j.ica.2011.03.060

di(chloromethyl)phosphinic acid, **L1** di(hydroxymethyl)phosphinic acid, **L2**

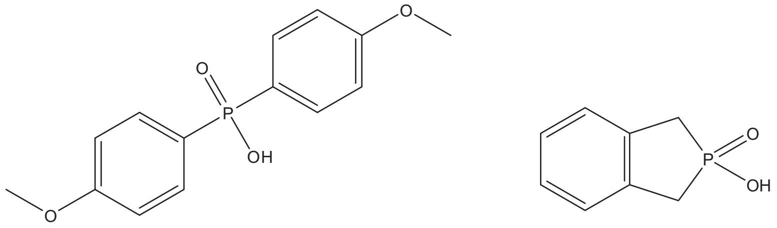

di(p-methoxyphenyl)phosphinic acid,**L3** 2-hydroxyisophosphindoline-2-oxide, **L4**

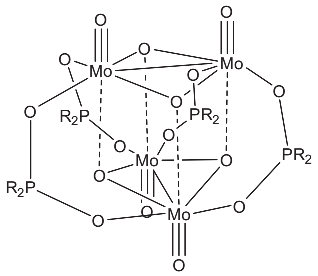

Scheme 1. Illustration of the four ligands and the resulting structure of the molybdenum tetramer produced using four conjugate bases of each ligand **L1**–**L4** to bind to the $[Mo_4O_8]^{4+}$ core producing complexes **1**–**4**, respectively.

tions. A Shimadzu QP5050 GC–MS was used for the mass spectra determinations and quantitative analysis for the epoxidation reactions. The elemental analysis data were obtained from Galbraith Laboratories, Inc, Knoxville, TN. Methylene chloride and *N*,*N*-diisopropylethylamine were dried from CaH_2 and NaH, respectively. Other solvents were used as received from commercial suppliers. Most chemicals were purchased from Aldrich and used as received. Di(chloromethyl)phosphinic acid [31,32] (**L1**), di(hydroxymethyl)phosphinic acid [31,32] (**L2**), and 2-hydroxyisophosphindoline-2-oxide [33] (**L4**) were prepared as described in the cited literature. Anilinium di(hydroxymethyl)phosphinate (**L2A**) was synthesized by refluxing an ethanol solution of ligand **L2** and aniline in the ratio of 1:1 for 2 h and then allowing the solution to cool to room temperature at which point colorless crystals formed.

2.2. Synthesis

2.2.1. Synthesis and characterization of tetramer $Mo_4(\mu^3\text{-}O)_4[\mu\text{-}O_2P(CH_2Cl)_2]_4O_4$, 1

Di(chloromethyl)phosphinic acid 0.15 g (0.92 mmol) was added to a solution of $MoO_2(acac)_2$ 0.30 g (0.92 mmol) in 8 mL of ethanol in a thick-walled tube. The tube was sealed with a Teflon cap and heated to 120 °C for 48 h. The mixture went through a green stage finally resulting in red crystals. This mixture was then cooled down to ambient temperature and filtered by vacuum filtration. Red crystals were collected and vacuum dried overnight affording 0.10 g of $Mo_4(\mu^3\text{-}O)_4[\mu\text{-}O_2P(CH_2Cl)_2]_4O_4$. Yield: 38% (based on Mo). *Anal.* Calc. for $C_8H_{16}Cl_8Mo_4O_{16}P_4$: C, 8.28; H, 1.39. Found: C, 8.44; H, 1.39%. ^{31}P NMR (THF): $\delta = 57.7$ ppm (s, 1P) relative to H_3PO_4. ^1H NMR (d_6-DMSO): $\delta = 3.39$ ppm (d, $ClCH_2P$, $J = 9.0$ Hz) IR (neat, cm^{-1}): 3014 (w), 2995 (w), 2940 (w), 1387 (m), 1225 (m), 1099 (m), 1015 (s), 977 (s), 847 (m), 779 (m), 715 (s), 663 (m) cm^{-1}.

2.2.2. Synthesis and characterization of $Mo_4(\mu^3\text{-}O)_4(\mu\text{-}O_2P(CH_2OH)_2)_4O_4$, 2

Di-(hydroxymethyl)phosphinic acid (0.12 g, 0.92 mmol) was added to a solution of $MoO_2(acac)_2$ (0.30 g, 0.92 mmol) in 7 ml of ethanol contained in a thick-walled tube. The tube was then sealed and heated to 120 °C for 48 h to obtain a red-brown precipitate. This mixture was cooled to ambient temperature and filtered. The precipitate was vacuum dried overnight affording 0.16 g (84%) of $Mo_4(\mu^3\text{-}O)_4(\mu\text{-}O_2P(CH_2OH)_2)_4O_4$. *Anal.* Calc. for $C_8H_{24}Mo_4O_{24}P_4\cdot 0.5(C_2H_5OH)$: C, 10.44; H, 2.63. Found: C, 10.66; H, 2.94%. ^1H NMR(d_6-DMSO): $\delta = 3.26$ ppm (d, $-CH_2P$, $J = 5.2$ Hz), $\delta = 3.55$(broad, s, $HO-CH_2$). ^{31}P NMR (DMSO): $\delta = 43.3$, 52.7 and 59.8 ppm. IR (neat, cm^{-1}): 3269 (broad, w), 2898 (w), 1420 (w), 1068 (w), 1008 (s), 966 (s), 851 (m), 723 (s) cm^{-1} .

2.2.3. Synthesis and characterization of $Mo_4(\mu^3\text{-}O)_4[\mu\text{-}O_2P(PhOMe)_2]_4O_4$, 3

Di(p-methoxyphenyl)phosphinic acid (0.26 g, 0.92 mmol) was mixed with $MoO_2(acac)_2$ (0.30 g, 0.92 mmol) in 7 ml ethanol using a similar procedure to that for compound **1** described above. The resulting red-orange precipitate was filtered and vacuum dried at room temperature for overnight affording 0.36 g of molybdenum tetramer **3** (Yield 97%). *Anal.* Calc. for $C_{56}H_{56}Mo_4O_{24}P_4.0.5(C_2H_5OH)$: C, 40.91; H, 3.43. Found: C, 40.67; H, 3.46%. ^{31}P NMR (CH_2Cl_2): $\delta = 47.6$ ppm (s, 1P) relative to H_3PO_4. IR (neat, cm^{-1}): 2993 (w), 2840 (w), 1596 (m), 1504 (m), 1299 (m), 1256 (m), 1128 (s) 1017 (s), 980(s), 836 (m), 805 (m), 711 (m), 671(m) cm^{-1}.

2.2.4. Synthesis and characterization of $Mo_4(\mu^3\text{-}O)_4[\mu\text{-}O_2P(o\text{-}C_6H_4(CH_2)_2)]_4O_4$, 4

0.034 g (0.1 mmol) of $MoO_2(acac)_2$ was added to 5 mL of ethanol in a thick-walled tube. The tube was sealed with a Teflon cap and heated to 120 °C for 4 h. It was then allowed to cool to room temperature and 0.018 g (1.1 mmol) of 2-hydroxyisophosphindoline-2-oxide was added to the solution. It was then heated to 120 °C for 36 h which resulted in the formation of a brown precipitate. The precipitate was filtered and then dissolved in methylene chloride. This solution was filtered to remove an insoluble byproduct to give a red filtrate. Hexanes were added to the filtrate and the solution was kept at 4 °C overnight. A red precipitate was collected the next day to afford 0.017 g of $Mo_4(\mu^3\text{-}O)_4[\mu\text{-}O_2P(o\text{-}C_6H_4(CH_2)_2)]_4O_4$. Yield: 50% (based on Mo). *Anal.* Calc. for $C_{32}H_{32}Mo_4O_{16}P_4$: C, 32.57; H, 2.73. Found: C, 32.98; H, 2.94%. ^{31}P NMR (CH_2Cl_2): $\delta = 88.3$ ppm (s, 1P) relative to H_3PO_4. ^1H NMR ($CDCl_3$): δ = 3.48-3.3.53 ppm (q, CH_2) δ = 7.27–7.33 ppm (m, C_6H_4).

2.3. X-ray crystallography

Suitable crystals of compound **1** were obtained by allowing the slow cooling of the reaction mixture. Red crystals of compound **4** suitable for single X-ray diffraction were obtained by dissolving the compound in dichloromethane, layering with hexanes, and allowing this mixture to stand for several days at room temperature. Suitable crystals of **L2A**, **L4**, **1** and **4** were coated with epoxy resin and mounted on a glass fiber. The instrument used was an Enraf-Nonius Turbo CAD4 X-ray diffractometer. Final cell constants and orientation matrix were obtained by collecting appropriate preliminary data, selecting 25 reflections, centering and refinement by a least squares fit, Table 1. Mo Kα radiation ($\lambda = 0.71073$ Å) was used for data collection. The procedures used to collect the data, solve and refine the structure were as detailed previously for other complexes [30].

2.4. Epoxidation of cis-cyclooctene in the presence of H_2O_2

The reactions were carried out under an open atmosphere using a two-necked 25 ml round bottom flask equipped with a reflux condenser and a magnetic stirrer. In a typical experiment, 1.82 mmol of *cis*-cyclooctene, 1 mol % catalyst (1.82×10^{-2} mmol), 2.0 mL ethanol, 0.28 ml of 30% H_2O_2 (2.72 mmol, 1.5 equiv.), and 0.100 g n-decane (0.703 mmol) as an internal standard were mixed together and the mixture heated to 70 °C. Samples were taken periodically and analyzed by a Shimadzu QP5050 GC–MS. The conversion and the selectivity of the reaction were calculated using calibration curves.

3. Results and discussion

3.1. Synthesis and spectral characterization

We have previously reported that $Mo_4(\mu^3\text{-}O)_4[\mu\text{-}O_2P(Ph)_2]_4O_4$ can be produced by heating an ethanol solution of $MoO_2(acac)_2$ with diphenylphosphinic acid at 120 °C in a Teflon capped glass tube for 48 hours [30]. Compounds **1**, **3** and **4** were prepared by following a similar procedure substituting the appropriate ligand in place of diphenylphosphinic acid. Compounds **1**, **3**, and **4** were characterized by ^1H NMR, ^{31}P NMR, IR and UV–Vis spectroscopy.

Compound **2** on the other hand proved to be much harder to synthesize. A red precipitate was obtained after heating $MoO_2(acac)_2$ with ligand **L2** in ethanol for 48 h. The IR spectrum of this product showed the signature stretching mode for a single Mo≡O bond at 966 cm^{-1} which is in agreement with other molybdenum tetramers. The bands at 3269 and 1068 cm^{-1} can be assigned to O–H and P═O stretches, respectively. The proton NMR spectrum of **2** has a doublet at 3.26 ppm and a broad singlet at 3.55 ppm which are due to the presence of hydrogen atoms on the methyl group and hydroxyl group, respectively. The ^{31}P NMR spectrum of **2** puzzled us as it consisted of several resonances ranging from 43.3 to 59.8 ppm. This indicates that precipitate **2** may be a mixture of several molybdenum compounds. The mixture of **2** was imputed

Table 1
Crystal data and structure refinement details of ligands **L2A**, **L4**, **1** and **4**.

Compound	**L2A**	**L4**	**1**	**4**
Molecular formula	$C_8H_{14}NO_4P$	$C_8H_9O_2P$	$C_8H_{16}Cl_8Mo_4O_{16}P_4$	$C_{32}H_{32}Mo_4O_{16}P_4$
Formula weight	219.17	168.12	1159.45	1180.22
Crystal size (mm)	0.50 × 0.40 × 0.20	0.45x0.30x0.30	0.25x0.15x0.05	0.20x0.20x0.10
Crystal color	colorless	Colorless	Red-Brown	Red
T (K)	291(2)	291(2)	291(2)	291(2)
Crystal system	monoclinic	Monoclinic	Triclinic	Triclinic
Space group	*P*2(1)/C	*P*2(1)/C	$P\bar{1}$	$P\bar{1}$
a (Å)	11.909(3)	8.843(3)	8.979(3)	12.796(2)
b (Å)	8.555(5)	8.139(2)	9.379(5)	13.751(4)
c (Å)	11.304(3)	11.788(3)	19.120(10)	13.816(2)
α (°)	90	90	101.34(4)	111.25(2)
β (°)	110.72(2)	107.70(2)	100.39(4)	110.19(1)
γ (°)	90	90	98.81(4)	102.63(2)
V (Å)^3	1077.2(7)	808.3(4)	1522.9(12)	1955.5(9)
Z	4	4	2	2
D_{calc} (g/cm^3)	1.351	1.382	2.529	2.004
Absorption coefficient (mm^{-1})	0.245	0.283	2.585	1.488
F(0 0 0)	464	352	1112	1160
θ (°)	1.83–22.47	2.42–24.97	1.11–22.47	1.73–22.47
Number of reflections measured	1401	1412	4268	5387
Number of observed data [$I > 2\sigma(I)$]	1202	1232	3962	5109
Number of parameters	145	104	361	505
R_1,[a] wR_2 [$I > 2\sigma(I)$][b]	0.056, 0.143[c]	0.032, 0.078[d]	0.066, 0.173[e]	0.023, 0.062[f]
R_1, wR_2 (all data)	0.064, 0.153	0.039, 0.083	0.087, 0.196	0.029, 0.065
Goodness-of-fit (GOF) on F^2	1.056	1.055	1.106	1.096

[a] $R_1 = \Sigma||F_o| - |F_c||/\Sigma|F_o|$.

[b] $wR_2 = [\Sigma[w(F_o{}^2 - F_c{}^2)^2]/\Sigma[w(F_o{}^2)^2]]^{1/2}$.

[c] $w = 1/[{}^2(F_o{}^2)+(0.1082P)^2 + 0.5002P]$ where $P = (F_o{}^2 + 2(F_c)^2)/3$.

[d] $w = 1/[{}^2(F_o{}^2)+(0.0313P)^2 + 0.4430P]$.

[e] $w = 1/[{}^2(F_o{}^2)+(0.0853P)^2 + 52.5061P]$.

[f] $w = 1/[{}^2(F_o{}^2)+(0.0375P)^2 + 1.3582P]$.

Table 2
^{31}P NMR chemical shift of ligands **L1**–**L4**, **L2A** and compounds **1**–**4** at 25 °C.

Compound	^{31}P NMR (ppm)[a], (solvent)
$(ClCH_2)_2POOH$, **L1**	36.0 (s), (THF)
$(HOCH_2)_2POOH$, **L2**	45.9 (s), (D_2O)
$(MeOPh)_2POOH$, **L3**	33.4 (s), (CH_2Cl_2)
$(o\text{-}C_6H_4(CH_2)_2POOH$, **L4**	73.1 (s), ($CDCl_3$)
$PhNH_3[OOP(HOCH_2)_2]$, **L2A**	42.7 (s), (EtOH)
$Mo_4(\mu^3\text{-}O)_4[\mu\text{-}O_2P(CH2Cl)_2]_4O_4$, **1**	57.7 (s), (THF)
$Mo_4(\mu^3\text{-}O)_4[\mu\text{-}O_2P(CH_2OH)_2)_4O_4$, **2**	43.3, 52.7, 59.8 (m), (DMSO)
$Mo_4(\mu^3\text{-}O)_4[\mu\text{-}O_2P(PhOMe)_2]_4O_4$, **3**	47.6 (s) , (CH_2Cl_2)
$Mo_4(\mu^3\text{-}O)_4[\mu\text{-}O_2P(o\text{-}C_6H_4(CH_2)_2)]_4O_4$, **4**	88.3(s), (CH_2Cl_2)

[a] s = singlet, m = multiple resonances.

initially to an impurity in ligand **L2** (95% pure based on ^{31}P NMR). The anilinium salt of ligand **L2** (**L2A**) was then made by refluxing aniline with ligand **L2** in ethanol for two hours and this compound was then employed to make **2** by heating a mixture of $MoO_2(acac)_2$ and **L2A** in ethanol. In this case, the ^{31}P NMR spectrum contained resonances ranging from 43.3 to 62.6 ppm. This suggests that a mixture of products was produced even using pure **L2A**. Corcoran and Haushalter have reported 1D and 2D molybdenum phosphate polymers were produced hydrothermally by mixing different molybdenum sources with phosphoric acid under different reaction conditions [25,28]. Also, like phosphoric acid, ligand **L2** has four active oxygen atoms which can bind to the molybdenum center. Different coordination modes of ligand **L2** may be the reason for the resonances in the ^{31}P NMR spectrum of **2** since a reasonable elemental analysis was obtained. We have not been able to obtain a ^{31}P NMR spectroscopically pure sample of **2** despite employing several different synthetic routes [20,23,25].

The ^{31}P chemical shifts of the ligands and compounds are listed in Table 2. Free ligands **L1**–**L4** and **L2A** resonate at 36.0, 45.9, 33.6, 73.1 and 42.7 ppm, respectively. A single resonance was observed for **1**, **3**, and **4** at the position of 57.7, 47.6 and 88.4 ppm, respectively. The downshifts of the resonance peaks of the coordinated ligands from the free ligands are comparable to what was observed previously [30]. In addition, a doublet at 3.39 ppm and a quartet at 3.51 ppm were observed in the ^{1}H NMR spectrum of **1** and **4**, respectively which are due to the H-atoms on the methylene groups.

The IR spectra of compounds **1**, **3** and **4** contain diagnostic bands at 977, 980 and 980 cm^{-1}, respectively indicating the stretching mode for $\nu(Mo{=}O)$. The bands at 1125, 1128 and 1130 cm^{-1} for compounds **1**, **3** and **4** can be ascribed to the $\nu(P{=}O)$ stretch which are blue shifted compared to the free ligands. Absorptions for **1**, 308; **2**, 308; **3**, 316; **4**, 308 nm are observed for compounds **1**–**4** in DMSO which can be attributed to ligand to metal charge transitions. There are bigger differences observed in the weaker absorptions ascribed to d-d transitions (presumably σ to σ^* transitions) with **1**, 482 nm; **2**, 489 nm; **3**, 467 nm, **4**, 472 nm. This is perhaps related to the ability of the ligand to donate electron density to the Mo atoms allowing for good overlap in the Mo–Mo single bond as the more electronegative ligands in complexes **1** and **2** would appear to have a slightly weaker interaction *in DMSO solution*.

*3.2. X-ray crystallographic data of $C_6H_5NH_3.O_2P(CH_2OH)_2$, **L2A** and $C_8H_8PO_2H$, L4*

Colorless crystals of ligand **L2A** suitable for single X-ray diffraction were obtained by cooling an ethanol solution of the compound overnight in a refrigerator. Colorless crystals of **L4** were grown by putting a saturated acetone solution in the freezer overnight. Selected bond lengths and angles of compound **L2A** and **L4** and a listing of hydrogen bonds are given in Tables 3 and 4, respectively.

Table 3
Selected bond distances (Å) and angles (°) for ligands **L2A** and **L4**.

L2A		**L4**	
Bond distances (Å)			
P(1)–O(1)	1.507(2)	O(1)–P(1)	1.552(2)
P(1)–O(2)	1.510(2)	O(2)–P(1)	1.485(2)
P(1)–C(1)	1.807(4)	C(7)–P(1)	1.800(2)
P(1)–C(2)	1.811(4)	C(8)–P(1)	1.796(2)
C(1)–O(4)	1.396(5)		
C(2)–O(3)	1.425(4)		
N(1)–C(3)	1.452(4)		
Bond angles (°)			
O(1)–P(1)–O(2)	116.22(14)	O(2)–P(1)–O(1)	113.22(9)
O(1)–P(1)–C(1)	110.71(16)	O(2)–P(1)–C(8)	115.83(10)
O(2)–P(1)–C(1)	106.66(15)	O(1)–P(1)–C(8)	107.99(9)
O(1)–P(1)–C(2)	107.04(14)	O(2)–P(1)–C(7)	116.52(10)
O(2)–P(1)–C(2)	109.12(15)	O(1)–P(1)–C(7)	104.46(10)
C(1)–P(1)–C(2)	106.72(17)	C(8)–P(1)–C(7)	97.12(9)
O(4)–C(1)–P(1)	111.6(2)	C(1)–C(7)–P(1)	104.06(13)
O(3)–C(2)–P(1)	112.0(2)		

Table 4
Hydrogen bonds for **L2A** and **L4** with H···A < r(A) + 2.000 Å) and ⟨DHA⟩ 110°.

D–H···A	d(D–H)	d(H···A)	d(D···A)	⟨(DHA)
L2A				
N1-–H1C···O2[a]	0.88(5)	1.84(5)	2.721(5)	174(4)
N1-–H1D···O3[b]	1.00(4)	1.82(4)	2.810(4)	172(3)
N1-–H1E···O1[c]	0.91(3)	1.78(3)	2.684(5)	174(4)
O3–H3···O2[a]	0.82(6)	1.84(6)	2.649(4)	173(6)
O4–H4A···O1[d]	0.79(5)	2.02(6)	2.775(4)	161(5)
L4				
O1–H1···O2[e]	0.84(3)	1.70(3)	2.521(2)	167(3)

Symmetry transformations used to generate equivalent atoms:
[a] $1-x, -1/2+y, 1/2-z$.
[b] $x, 1/2-y, 1/2+z$.
[c] $x, -1+y, z$.
[d] $x, 3/2-y, 1/2+z$.
[e] $-x, 1/2+y, 1/2-z$.

An ORTEP-3 [34] drawing of ligand **L2A** is shown in Fig. 1. Four molecules of **L2A** crystallized in a monoclinic unit cell. The phosphorous atom is in a distorted tetrahedral geometry with the O–P–O and C–P–C bond angles equal to 116.22(14) and 106.72(17)°, respectively. The bond angles for O–P–C range from 106.66(15) to 110.71(16)° due to the different coordination environments among oxygen atoms. The P–O bond distances at 1.507(2) and 1.510(2) Å are not significantly different, are intermediate between expected values for P=O and P–O bond lengths [35,36] and suggestive of a multiple bond. A large degree of hydrogen bonding occurred in the crystal packing of **L2A**. In the refinement of this molecule, the five H atoms involved in H-bonding were freely refined (includes the three H atoms on the N atom) except for the two attached to O atoms (on the OH moiety) which had only their thermal parameters constrained. Two of the H atoms attached to the N atom are each H-bonded to two phosphinate O atoms and the remaining H atom is H-bonded to OH groups on adjacent anions as listed in Table 4 and illustrated in Fig. S1. As can be seen in the labeled anion in Fig. S1, the phosphinate O atoms are also H-bonded to an OH moiety on an adjacent phosphinate as well as to the H-atoms on the N atom on the anilinium cation. This results in an interconnected planar 2-dimensional array of molecules held together with these H-bonds which are stacked up parallel to each other resulting in polar and nonpolar domains in the crystal, see Fig. S2.

An ORTEP-3 [34] representation of ligand **L4** is illustrated in Fig. 2. Ligand **L4** crystallizes in a monoclinic unit cell. The bond

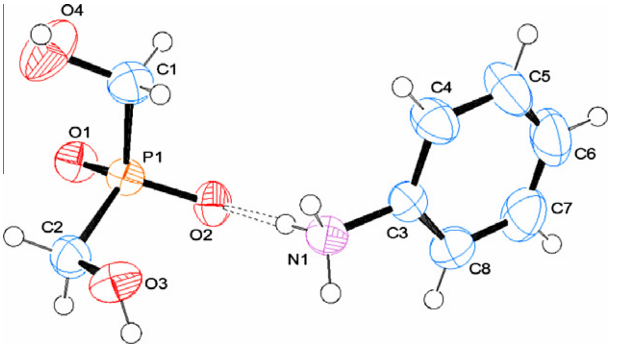

Fig. 1. ORTEP-3 [34] representation of **L2A** with selected atom numbering. Thermal ellipsoids are drawn at the 50% probability level and hydrogen atoms are represented by circles of arbitrary radii. One H-bond is illustrated with a dashed line.

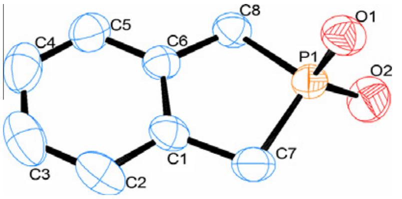

Fig. 2. ORTEP-3 [34] representation of **L4** with selected atom numbering. Thermal ellipsoids are drawn at the 50% probability level and hydrogen atoms are not shown.

angles at the phosphorous atom range from 97.12(9)° to 116.52(10)°, with the lowest angle being for the C–P–P angle. There are two significantly different P–O bond distances; the short $P{=}O_2$ and longer P–(O1)–H which are 1.485(2) and 1.552(2) Å, respectively. These values are in good agreement with the average P=O and P–OH distances found in other organic phosphates [35–40]. An infinite one dimensional chain was formed by inter molecular hydrogen bonding between the (O1)–H and O2 atoms as shown in Fig. S3. In this case the H atom bonded to O1 was refined freely and the rest constrained. The O1–O2 bond length and angle for O2···H–O1 are 2.521(2) Å and 167(3)°, respectively, see Table 4.

3.3. X-ray crystallographic data of $Mo_4(\mu^3\text{-}O)_4[\mu\text{-}O_2P(CH2Cl)_2]_4O_4$, **1** and $Mo_4(\mu^3\text{-}O)_4[\mu\text{-}O_2P(o\text{-}C_6H_4(CH_2)_2)]_4O_4$, **4**

Crystal data and details of structural refinement for compounds **1** and **4** are listed in Table 1. ORTEP [34] representations of compounds **1** and **4** are shown in Figs. 3 and 4. Both **1** and **4** crystallized in the triclinic space group $P\bar{1}$ with one entire molecule of each comprising the asymmetric unit. The structures of **1** and **4** consist of distorted $[Mo_4O_4(\mu^3\text{-}O)_4]^{4+}$ cubic cores which are assembled by two $[Mo_2O_4]^{2+}$ units and four bridging phosphinate ligands attached to four of the six cubic faces. Distances and angles corresponding to one of these $[Mo_2O_4]^{2+}$ units are listed in Tables 5 and 6, respectively for **1** and **4**. The other halves, while not identical, are not different enough to warrant inclusion and can be obtained from the CIF files. Each molybdenum atom is coordinated in a distorted octahedral fashion by six oxygen atoms: one terminal triply-bonded oxygen atom, three μ^3-bridging oxygen atoms, and two oxygen atoms from two different ligands. The bond lengths of the molybdenyl group ($Mo{\equiv}O$) range from 1.661(10)–1.669(11) and 1.657(2)–1.668(3) Å for **1** and **4**, respectively. Much longer interactions were found for the Mo···O bonds in the position *trans* to the molybdenyl group ranging from 2.366(11) to 2.443(11) Å in **1** and 2.412(3)–2.430(3) Å for **4**. These large Mo···O(oxo) interactions are caused by the *trans* effect of the triply-bonded terminal oxo ligands [25,27,30]. The Mo–O(oxo) bond distances on the

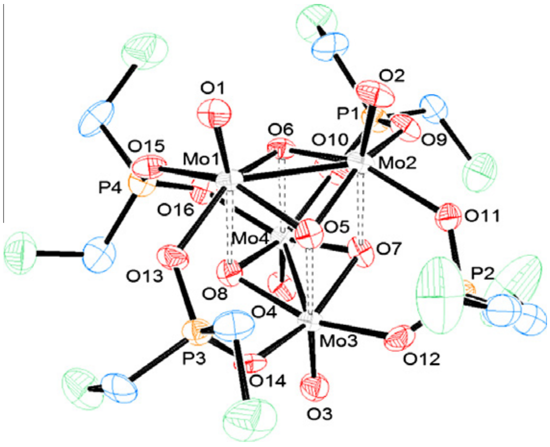

Fig. 3. ORTEP-3 [34] representation of **1** with selected atom numbering. Thermal ellipsoids are drawn at the 50% probability level and hydrogen atoms are omitted for clarity.

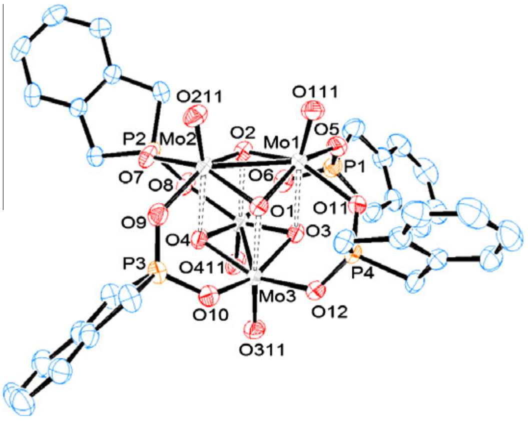

Fig. 4. ORTEP-3 [34] representation of **4** with selected atom numbering. Thermal ellipsoids are drawn at the 50% probability level and hydrogen atoms are omitted for clarity.

Table 5
Selected bond distances (Å) for compounds **1** and **4**.

Compound 1		Compound 4	
Mo(1)–O(1)	1.668(11)	Mo(1)–O(111)	1.657(2)
Mo(1)–O(5)	1.933(10)	Mo(1)–O(2)	1.965(2)
Mo(1)–O(6)	1.954(10)	Mo(1)–O(1)	1.968(2)
Mo(1)–O(15)	2.058(11)	Mo(1)–O(5)	2.057(2)
Mo(1)–O(13)	2.065(10)	Mo(1)–O(11)	2.072(2)
Mo(1)···O(8)	2.443(11)	Mo(1)···O(3)	2.430(3)
Mo(1)–Mo(2)	2.629(2)	Mo(1)–Mo(2)	2.6433(6)
Mo(2)–O(2)	1.661(10)	Mo(2)–O(211)	1.666(2)
Mo(2)–O(6)	1.940(10)	Mo(2)–O(2)	1.958(2)
Mo(2)–O(5)	1.971(10)	Mo(2)–O(1)	1.961(2)
Mo(2)–O(11)	2.074(11)	Mo(2)–O(7)	2.062(2)
Mo(2)–O(9)	2.082(10)	Mo(2)–O(9)	2.085(2)
Mo(2)···O(7)	2.378(11)	Mo(2)···O(4)	2.412(3)
Mo(3)–Mo(4)	2.624(2)	Mo(3)–Mo(4)	2.6264(7)
O(9)–P(1)	1.490(11)	O(5)–P(1)	1.523(3)
O(10)–P(1)	1.536(11)	O(6)–P(1)	1.542(3)
O(11)–P(2)	1.508(11)	O(7)–P(2)	1.529(3)
O(12)–P(2)	1.499(12)	O(8)–P(2)	1.526(3)
O(13)–P(3)	1.522(11)	O(9)–P(3)	1.525(3)
O(14)–P(3)	1.487(12)	O(10)–P(3)	1.533(3)
O(15)–P(4)	1.507(11)	O(11)–P(4)	1.529(3)
O(16)–P(4)	1.523(12)	O(12)–P(4)	1.526(3)

Table 6
Selected bond angles (°) for compounds **1** and **4**.

Compound **1**		Compound **4**	
O(1)–Mo(1)–O(5)	110.5(5)	O(111)–Mo(1)–O(2)	111.28(11)
O(1)–Mo(1)–O(6)	109.6(5)	O(111)–Mo(1)–O(1)	109.34(11)
O(5)–Mo(1)–O(6)	88.9(4)	O(2)–Mo(1)–O(1)	88.71(10)
O(1)–Mo(1)–O(15)	98.4(5)	O(111)–Mo(1)–O(5)	98.62(11)
O(5)–Mo(1)–O(15)	150.7(4)	O(2)–Mo(1)–O(5)	84.77(10)
O(6)–Mo(1)–O(15)	85.3(4)	O(1)–Mo(1)–O(5)	151.75(10)
O(1)–Mo(1)–O(13)	98.5(5)	O(111)–Mo(1)–O(11)	98.03(11)
O(5)–Mo(1)–O(13)	83.7(4)	O(2)–Mo(1)–O(11)	150.61(10)
O(6)–Mo(1)–O(13)	151.7(4)	O(1)–Mo(1)–O(11)	83.45(9)
O(15)–Mo(1)–O(13)	88.0(4)	O(5)–Mo(1)–O(11)	88.87(10)
O(1)–Mo(1)–O(8)	169.9(5)	O(111)–Mo(1)–O(3)	169.43(10)
O(5)–Mo(1)–O(8)	77.0(4)	O(2)–Mo(1)–O(3)	76.95(9)
O(6)–Mo(1)–O(8)	76.5(4)	O(1)–Mo(1)–O(3)	76.72(9)
O(15)–Mo(1)–O(8)	73.7(4)	O(5)–Mo(1)–O(3)	75.03(9)
O(13)–Mo(1)–O(8)	75.3(4)	O(11)–Mo(1)–O(3)	73.69(9)
O(1)–Mo(1)–Mo(2)	98.9(4)	O(111)–Mo(1)–Mo(2)	99.69(9)
O(8)–Mo(1)–Mo(2)	91.1(2)	O(3)–Mo(1)–Mo(2)	90.78(6)
O(2)–Mo(2)–O(6)	110.2(5)	O(211)–Mo(2)–O(2)	110.65(12)
O(2)–Mo(2)–O(5)	109.2(5)	O(211)–Mo(2)–O(1)	109.30(11)
O(6)–Mo(2)–O(5)	88.2(4)	O(2)–Mo(2)–O(1)	89.12(10)
O(2)–Mo(2)–O(11)	97.1(5)	O(211)–Mo(2)–O(7)	98.92(11)
O(6)–Mo(2)–O(11)	152.4(4)	O(2)–Mo(2)–O(7)	83.83(10)
O(5)–Mo(2)–O(11)	86.2(4)	O(1)–Mo(2)–O(7)	151.59(10)
O(2)–Mo(2)–O(9)	98.0(5)	O(211)–Mo(2)–O(9)	96.41(12)
O(6)–Mo(2)–O(9)	82.8(4)	O(2)–Mo(2)–O(9)	152.74(10)
O(5)–Mo(2)–O(9)	152.8(4)	O(1)–Mo(2)–O(9)	84.90(9)
O(11)–Mo(2)–O(9)	90.0(4)	O(7)–Mo(2)–O(9)	88.88(10)
O(2)–Mo(2)–O(7)	169.6(5)	O(211)–Mo(2)–O(4)	169.16(11)
O(6)–Mo(2)–O(7)	77.1(4)	O(2)–Mo(2)–O(4)	77.48(9)
O(5)–Mo(2)–O(7)	77.7(4)	O(1)–Mo(2)–O(4)	77.27(9)
O(11)–Mo(2)–O(7)	75.3(4)	O(7)–Mo(2)–O(4)	74.34(9)
O(9)–Mo(2)–O(7)	75.3(4)	O(9)–Mo(2)–O(4)	75.26(9)
O(2)–Mo(2)–Mo(1)	98.4(4)	O(211)–Mo(2)–Mo(1)	99.16(9)
O(7)–Mo(2)–Mo(1)	91.9(3)	O(4)–Mo(2)–Mo(1)	91.63(6)
Mo(1)–O(5)–Mo(2)	84.6(4)	Mo(2)–O(1)–Mo(1)	84.54(9)
Mo(1)–O(5)–Mo(3)	104.2(4)	Mo(2)–O(1)–Mo(3)	102.54(10)
Mo(2)–O(5)–Mo(3)	101.9(4)	Mo(1)–O(1)–Mo(3)	102.92(10)
Mo(2)–O(6)–Mo(1)	84.9(4)	Mo(2)–O(2)–Mo(1)	84.70(9)
Mo(2)–O(6)–Mo(4)	103.0(4)	Mo(2)–O(2)–Mo(4)	102.43(10)
Mo(1)–O(6)–Mo(4)	103.4(4)	Mo(1)–O(2)–Mo(4)	102.79(10)
P(1)–O(9)–Mo(2)	127.8(7)	P(1)–O(5)–Mo(1)	130.44(15)
P(2)–O(11)–Mo(2)	132.3(6)	P(2)–O(7)–Mo(2)	127.85(14)
P(3)–O(13)–Mo(1)	128.7(7)	P(3)–O(9)–Mo(2)	129.71(14)
P(4)–O(15)–Mo(1)	132.1(7)	P(4)–O(11)–Mo(1)	125.27(14)
O(9)–P(1)–O(10)	115.6(6)	O(5)–P(1)–O(6)	114.03(14)

equatorial plane range from 1.933(10) to 1.971(10) Å and 1.951(2) to 1.968(2) Å for **1** and **4**, respectively and are shorter than the Mo–O(phosphinate) bond distances which range from 2.058(11) to 2.088(11) Å in **1** and 2.057(2)–2.085(2) Å for **4**. There is a greater range in P–O bond distances in **1** at 1.49(1)–1.54(1) Å compared to the range in **4** at 1.523((3)–1.542(3) Å though the average P–O bond distances on **1** at 1.51(2) Å is not significantly different than that on **4** at 1.529(6) Å.

The $[Mo_4O_4(\mu^3\text{-}O)_4]^{4+}$ cubes in **1** and **4** also contain two Mo–Mo single bonds; similar bond distances for **1** at 2.629(2) and 2.624(2) Å and significantly different ones in **4** at 2.6433(6) and 2.6264(7) Å. The non-bonded Mo···Mo distances range from Mo(2)···Mo(3) = 3.378(2) Å to Mo(1)···Mo(4) = 3.421(2) Å for **1** and Mo(2)···Mo(4) = 3.4232(5) Å to Mo(1)···Mo(3) = 3.4379(4) Å for **4**. Therefore some equivalent Mo–Mo bond distances and non-bonded interactions in **1** are significantly shorter than those in **4** indicating that **1** is a smaller cube. This conclusion is also supported by the fact that three of the long Mo···O(oxo) interactions which connect the two $[Mo_2O_4]^{2+}$ units in **1** are significantly shorter than those in **4**; specifically Mo(2)···O(7) = 2.378(11) Å, Mo(3)···O(5) = 2.366(11) Å, Mo(4)···O(6) = 2.389(10) Å in **1** are all significantly shorter than the equivalent in **4** of Mo(2)···O(4) = 2.412(3) Å, Mo(3)···O(1) = 2.413(2) Å, Mo(4)···O(2) = 2.418(3) Å with comparable Mo(1)···O(8) = 2.443(11) Å in **1** longer than Mo(1)···O(3) = 2.430(3) Å in **4**. The difference may arise out of crystal packing forces as the phenyl substituents in **4** enforce a more rigid environment around the donating $R_2PO_2^-$ entity and may be forced to twist in order to minimize steric forces resulting in an elongation of the cube. The Mo–Mo bond distances are similar with those in molybdenum tetramers previously reported [30], but are significantly longer than those in $[Mo_4O_8(C_4O_4)]^{4-}$, i.e., Mo1–Mo2 = 2.5904(4) Å and Mo3–Mo4 = 2.5932(4) Å [27], $[Mo_4O_4(\mu_3\text{-}O)_4(OSi(Me)_3)_4(HN(Me)_2]_4$, i.e., Mo1–Mo2 = 2.607(4) and Mo3–Mo4 = 2.606(4) Å [26].

There are two different bond angles within each $[Mo_2O_4]^{2+}$ unit of the $[Mo_4O_4(\mu^3\text{-}O)_4]^{4+}$ cube. The Mo–μ^3-O–Mo angles range from 84.3(4) to 104.2(4)° and 84.33(9) to 102.83(10)° for **1** and **4**, respectively which are not significantly different. The other one involving the Mo atoms at the center (i.e., μ^3-O–Mo–μ^3-O) range from 76.5(4) to 110.5(5)° for **1** and 76.72(9)–111.28(11)° for **4** are also not significantly different suggesting that the $[Mo_2O_4]^{2+}$ units in **1** and **4** are similar.

3.4. Application in epoxidation catalysis

Molybdenum complexes are used as catalysts for the epoxidation of olefins with tert-butyl hydrogen peroxide in non-aqueous solvents. However, efficient Mo catalysts with H_2O_2 as the source of oxygen are limited [11,12,41–45] either because the presence of water poisons the catalyst [46] or the use of H_2O_2 reduces the catalytic activities or selectivies [47]. We did previously report on the catalytic potential of molybdenum or tungsten monomeric compounds such as $MO_2Cl_2(OPPh_2Me)_2$, $MO_2Cl_2dppmO_2$, and $MO_2Cl_2(OPPh_2CH_2OH)_2$ (M = Mo or W) in the presence of H_2O_2 which displayed high activity and selectivity [11,12]. We have now extended our investigation to molybdenum tetramers **1** through **4** and the previously prepared $Mo_4(\mu^3\text{-}O)_4[\mu\text{-}O_2P(CH_2C_6H_5)_2]_4O_4$, **5** [48] and $Mo_4(\mu^3\text{-}O)_4[\mu\text{-}O_2P(C_6H_5)_2]_4O_4$, **6** [30]. In order to compare

Table 7
Epoxidation of *cis*-cyclooctene with catalysts in the presence of H_2O_2 in ethanol solvent.[a].

Entry	Catalyst	Cyclooctene epoxide yield (%)		TOF[b] (mol mol cat^{-1} h^{-1})
		6h	24h	
1	Compound **1**	33.8	83.4	2.9
2	Compound **2**	54.8	90.8	26.8
3	Compound **3**	1.7	32.5	0
4	Compound **4**	28.6	44.7	1.8
5	$Mo_4(\mu^3\text{-}O)_4[\mu\text{-}O_2P(CH_2C_6H_5)_2]_4O_4$, **5**[c]	2.5	16.2	0
6	$Mo_4(\mu^3\text{-}O)_4[\mu\text{-}O_2P(C_6H_5)_2]_4O_4$, **6**[d]	ND[e]	<1	0

[a] Experiment condition: catalyst/*cis*-cyclooctene/H_2O_2 mole ratio equals 1:100:150. $T = 70$ °C. GC–MS quantitative analysis using decane as internal standard.

[b] The TOF were calculated after 30 min reaction time and described as mol epoxide/mol catalyst time (h).

[c] Ref. [48].

[d] Ref. [30].

[e] None detected.

the catalytic attributes of these molybdenum compounds with that of related compounds made before, the reactions were carried out using conditions identical to those utilized previously [11,12].

The results for the epoxidation of *cis*-cyclooctene with the ethanol/H_2O_2 system using complexes **1**–**4**, **5** and **6** as catalysts are summarized in Table 7. It should be noted that all reactions are remarkably clean as only the epoxide was the final produced. Control experiments confirmed that none of epoxide was detected in the absence of catalyst. It is clear from the results listed in Table 7 that compound **2** has the highest initial catalytic activity (TOF = 26.8) compared to other compounds. In contrast, none of the epoxide was detected after 30 min when compounds **3**, **5** and **6** were used as catalysts. Compound **2** kept its high efficiency and resulted in 54.8% conversion to the epoxide after 6 h and reached 90.8% after 24 h. Interestingly the TOF and conversion to the epoxide for compounds **1** and **4** are not significantly different after 6 h. However, 83.4% of the epoxide was produced after 24 h for compound **1** which is almost twice as much as that of compound **4**. Compound **3** has the lowest catalytic property among the compounds **1**–**4**, and resulted in 32.5% epoxide after 24 h. The catalytic potential of the previously reported **5** and **6** was also evaluated under identical conditions. Almost no catalytic activity was found for compound **6**. Complex **5** showed slightly better catalytic activity than **6** as 16.2% epoxide conversion was noted after 24 h. A clear orange/red solution was obtained when compound **1** or **2** was used in the catalytic reaction. However, compounds **3–6** all resulted in an orange/red suspension in the ethanol/H_2O_2 system. The big difference in catalytic activity may be attributed to the better solubility of **1** and **2** in the ethanol/H_2O_2 system. Other reported monomeric molybdenum complexes such as $Mo(O)_2(Cl)_2(OPMePh_2)_2$, $Mo(O)_2(Cl)_2dppmO_2$ [11] and $MoO_2Cl_2(OPPh_2CH_2OH)_2$ [12] resulted in 43%, 26% and 36.5%, respectively after 6 h under similar conditions and the yield of epoxide remained constant for $Mo(O)_2(Cl)_2(OPMePh_2)_2$ and $Mo(O)_2(Cl)_2dppmO_2$ even with longer reaction times. The conversion to the epoxide only increased to 67.7% for $MoO_2Cl_2(OPPh_2CH_2OH)_2$ after 24 h. Compounds **1** and **2** appear to be the best epoxidation catalysts for *cis*-cyclooctene under these conditions.

The stability of the catalysts **1**–**4** was examined using ^{31}P NMR spectroscopy. The color of the reaction mixtures had changed to blue from orange/red and ^{31}P NMR spectra revealed that ligand dissociation occurred for compounds **1**, **2**, and **4** after 24 h in the ethanol/H_2O_2 system. The color of the reaction mixture for compounds **3**, **5** and **6** was unchanged after 24 h. This can also be attributed to the different solubilities for these compounds in the ethanol/H_2O_2 system since presumably if the complexes do not dissolve, they are not decomposing under the conditions for catalysis.

4. Conclusions

Several new molybdenum tetramers bearing functionalized organic phosphinates have been synthesized. Pure compounds **1**, **3** and **4** were prepared in good yields. However, despite reasonable elemental analyses, the precise nature of compound **2** has not yet been determined. We believe that the ligand μ-$O_2P(CH_2OH)_2$ is capable of exhibiting coordination isomerism in a bidentate mode binding either through the two phosphinate O atoms or via one of these atoms and an O atom from the hydroxyl group. Ligands **L2A**, **L4** and compounds **1** and **4** were also structurally characterized by single crystal X-ray diffraction. The crystal structure of **L2A** were built up from infinite 2D polymeric sheets formed via inter and intra hydrogen bonding among oxygen and nitrogen atoms. An infinite one dimensional polymeric chain was formed by inter molecular hydrogen bonding in **L4**. The ability of complexes **1**–**4** to catalyze the epoxidation of *cis*-cyclooctene in an ethanol/H_2O_2 system has been examined. Compounds **1** and **2** showed superior catalytic capability over **3** and **4**. This was attributed to the better solubility of these compounds under the "green" catalytic conditions.

Acknowledgements

We thank Michigan Technological University for supporting this research.

Appendix A. Supplementary material

CCDC 809490–809493 contain the supplementary crystallographic data for complexes **L2a**, **L4**, **1** and **4**, respectively. Figs. S1 and S2 depicting hydrogen bonding and unit cell packing for **L2A** and Fig. S3 showing the 1-D polymeric chain formed by **L4**. These data can be obtained free of charge from The Cambridge Crystallographic Data Centre via www.ccdc.cam.ac.uk/data_request/cif. Supplementary data associated with this article can be found, in the online version, at doi:10.1016/j.ica.2011.03.060.

References

[1] A.K. Yudin, Aziridines and Epoxides in Organic Synthesis, Weinheim, Wiley-VCH, 2006.
[2] K.A. Jorgensen, Chem. Rev. 89 (1989) 431.
[3] A.U. Barlan, A. Basak, H. Yamamoto, Angew. Chem., Int. Ed. Enl. 45 (2006) 5849.
[4] C. Freund, M. Abrantes, F.E. Kühn, J. Organomet. Chem. 691 (2006) 3718.
[5] F.R. Fronczek, R.L. Luck, G. Wang, Inorg. Chim. Acta 342 (2003) 247–254.
[6] F.E. Kühn, A.M. Santos, M. Abrantes, Chem. Rev. 106 (2006) 2455.
[7] G. Wang, L. Feng, R.L. Luck, D.G. Evans, Z. Wang, X. Duan, J. Mol. Catal. A: Chem. 241 (2005) 8.
[8] M. Herbert, A. Galindo, F. Montilla, Catal. Commun. 8 (2007) 987.
[9] S.K. Maiti, S. Dinda, S. Banerjee, A.K. Mukherjee, R. Bhattacharyya, Eur. J. Inorg. Chem. (2008) 2038.
[10] S.K. Maiti, K.M.A. Malik, S. Gupta, S. Chakraborty, A.K. Ganguli, A.K. Mukherjee, R. Bhattacharyya, Inorg. Chem. 45 (2006) 9843.
[11] A. Jimtaisong, R.L. Luck, Inorg. Chem. 45 (2006) 10391.
[12] L. Feng, E. Urnezius, R.L. Luck, J. Organomet. Chem. 693 (2008) 1564.
[13] J.C. Alonso, P. Neves, d.S.M.J. Pires, S. Quintal, P.D. Vaz, C. Silva, A.A. Valente, P. Ferreira, M.J. Calhorda, V. Felix, M.G.B. Drew, Organometallics 26 (2007) 5548.
[14] C.I. Fernandes, N.U. Silva, P.D. Vaz, T.G. Nunes, C.D. Nunes, Appl. Catal., A 384 (2010) 84.
[15] Y.-D. Li, X.-K. Fu, B.-W. Gong, X.-C. Zou, X.-B. Tu, J.-X. Chen, J. Mol. Catal. A: Chem. 322 (2010) 55.
[16] A. Rezaeifard, I. Sheikhshoaie, N. Monadi, M. Alipour, Polyhedron 29 (2010) 2703.
[17] J. Zhao, K.R. Jain, E. Herdtweck, F.E. Kuehn, Dalton Trans. (2007) 5567.
[18] K. Kamata, K. Yonehara, Y. Sumida, K. Yamaguchi, S. Hikichi, N. Mizuno, Science 300 (2003) 964.
[19] R. Noyori, M. Aok, K. Sato, Chem. Commun. (2003) 1977.
[20] J.J.C. Constable, P.J. Dunn, J.D. Hayler, G.R. Humphrey, J.L.J. Leazer, R.J. Linderman, K. Lorenz, J. Manley, B.A. Pearlman, A. Wells, A. Zaksh, T.Y. Zhang, Green Chem. 9 (2007) 411.
[21] A.S. Foust, L.F. Dahl, J. Am. Chem. Soc 92 (1970) 7337.
[22] T.R. Amarante, P.c. Neves, A.C. Coelho, S. Gago, A.A. Valente, F.A. Almeida Paz, M. Pillinger, I.S. Gonçalves, Organometallics 29 (2010) 883.
[23] P.D. Williams, M.D. Curtis, Inorg. Chem. 25 (1986) 4562.
[24] W. Schirmer, U. Floerke, H.J. Haupt, Z. Anorg. Allg. Chem. 574 (1989) 239.
[25] E.W. Corcoran, Inorg. Chem. 29 (1990) 157.
[26] G.S. Kim, D.A. Keszler, C.W. DeKock, Inorg. Chem. 30 (1991) 574.
[27] B. Modec, J.V. Brencic, E.M. Burkholder, J. Zubieta, Dalton Trans. (2003) 4618.
[28] L. Mundi, R.C. Haushalter, J. Am. Chem. Soc. 113 (1991) 6340.
[29] R. Mattes, K. Muehlsiepen, Z. Naturforsch, B: Anorg. Chem., Organ. Chem. 35B (1980) 265.
[30] A. Jimtaisong, L.S. Feng, S. Sreehari, C.A. Bayse, R.L. Luck, J. Cluster Sci. 19 (2008) 181.
[31] L. Maier, J. Organomet. Chem. 178 (1979) 157.
[32] P.W. Morgan, B.C. Herr, J. Am. Chem. Soc. 74 (1952) 4526.
[33] E.A. Boyd, M.E.K. Boyd, F. Kerrigan, Tetrahedron Lett. 37 (1996) 5425.
[34] L.J. Farrugia, J. Appl. Crystallogr. 1997 (1997) 565.
[35] M.E. Druyan, A.H. Reis Jr., E. Gebert, S.W. Peterson, G.W. Mason, D.F. Peppard, J. Am. Chem. Soc. 98 (1976) 4801.
[36] F. Giordano, A. Ripamonti, Acta Crystallogr., Sect. 22 (1967) 678.
[37] R.A. Sachleben, J.H. Burns, G.M. Brown, Inorg. Chem. 27 (1988) 1787.
[38] I.L. Karle, K. Britts, Acta Crystallogr., Sect. 20 (1966) 118.
[39] M. Calleri, J.C. Speakman, Acta Crystallogr., Sect. 17 (1964) 1097.
[40] R.P. Singh, B. Twamley, J.n.M. Shreeve, J. Chem. Soc., Dalton Trans. (2000) 4089.
[41] J. Li, G. Wang, Z. Shi, M. Yang, R.L. Luck, Struct. Chem. 20 (2009) 869.

[42] V.V.K.M. Kandepi, J.M.S. Cardoso, B. Royo, Catal. Lett. 136 (2010) 222.
[43] N. Gharah, S. Chakraborty, A.K. Mukherjee, R. Bhattacharyya, Chem. Commun. (2004) 2630.
[44] C. Dinoi, M. Ciclosi, E. Manoury, L. Maron, L. Perrin, R. Poli, Chem. Eur. J. 16 (2010) 9572. S9572/9571-S9572/9579.
[45] J.S. Costa, C.M. Markus, I. Mutikainen, P. Gamez, J. Reedijk, Inorg. Chim. Acta 363 (2010) 2046.
[46] M. Abrantes, A.M. Santos, J. Mink, F.E. Kuehn, C.C. Romao, Organometallics 22 (2003) 2112.
[47] A.M. Martins, C.C. Romao, M. Abrantes, M.C. Azevedo, J. Cui, A.R. Dias, M.T. Duarte, M.A. Lemos, T. Lourenco, R. Poli, Organometallics 24 (2005) 2582.
[48] J.S. Maass, M. Zeller, D. Holmes, C.A. Bayse, R.L. Luck, J. Cluster Sci. 22, doi:10.1007/s10876-011-0373-7.